

# **Evidence for Arctic Ozone Depletion in Late February and Early March 1994**

G. L. Manney, R. W. Zurek, L. Froidevaux, and J. W. Waters  
Jet Propulsion Laboratory/California Institute of Technology

Received \_\_\_\_\_; accepted \_\_\_\_\_

Submitted to *Geophysical Research Letters*, January 1995.

Short title: LATE WINTER 1994 ARCTIC OZONE DEPLETION

Abstract. Comparison of simulations of ozone transport using three-dimensional trajectory calculations with the ozone evolution observed by the Microwave Limb Sounder on the Upper Atmosphere Research Satellite provides strong evidence that substantial chemical ozone depletion occurred in the Arctic lower stratospheric vortex during late February and early March 1994. Dynamical processes, mainly diabatic descent, mask part of the chemical destruction of ozone. Over the thirty-day period studied, our calculations indicate that chemical destruction of ozone in the Arctic lower stratospheric vortex may have been as much as twice the observed ozone decrease.

## Introduction

Detection of chemical ozone depletion in the Arctic polar vortex is considerably more difficult than in the Antarctic. Because of higher northern polar temperatures, conditions in the Arctic vortex are favorable for the formation of polar stratospheric clouds (PSCs) and subsequent lower stratospheric chlorine activation] and ozone depletion for a much shorter time than in the southern hemisphere [e.g., *Manney and Zurek*, 1993]. In addition, the more active and distorted northern hemisphere (NH) vortex makes it considerably more difficult to separate dynamical and chemical effects. *Manney et al.* [1994a] analyzed ozone from the Microwave Limb Sounder (MLS) and nitrous oxide ( $\text{N}_2\text{O}$ ) from the Cryogen Limb Array Etalon Spectrometer (CLAES) on the Upper Atmosphere Research Satellite (UARS) to show strong evidence for chemical ozone depletion in the Arctic during February and early March 1993. Also for 1992-93, *Larsen et al.* [1994] analyzed ozone sonde and aerosol profiles at 2 sites in Greenland to detect chemical ozone depletion during the 1992-93 Arctic winter. Both studies used conservative tracer measurements ( $\text{N}_2\text{O}$  or aerosols) to indicate dynamical changes and found that the ozone behavior was inconsistent with those dynamical changes. *Manney et al.* [1995, submitted to *J. Atmos. Sci.*, hereafter M95] used three-dimensional trajectory calculations to further examine the transport of ozone during the Arctic winter of 1992-93 and contrasted observed with purely advected ozone distributions. These results indicated that significant chemical ozone loss occurred, with dynamical compensation masking up to  $\approx 30\%$  of the loss. *Larsen et al.* [1994] used aerosol measurements to infer diabatic descent and thus estimate the amount of chemical ozone destruction, with consistent results.

The lower stratospheric vortex was relatively warm through most of the 1993-94 NH winter, until a period of sudden cooling in late February (Fig. 1a shows minimum temperatures at 465 K). Minimum temperatures were slightly below the type 1 PSC formation threshold ( $\approx 195$  K) throughout January 1994, warming to slightly above it

in early February. MLS observed enhanced chlorine monoxide (ClO, the dominant form of reactive chlorine that destroys ozone) in early February, with a subsequent decrease until the late February drop in temperatures; ClO was then observed to increase [Waters *et al.*, 1995]. Fig. 1b shows “vortex-averaged” [Manney *et al.*, 1995] MLS ozone in the lower stratosphere from mid-February through mid-March 1994. Average ozone on isentropic surfaces decreases below  $\approx 450$  K in the early part of the period; a larger and more general decrease over most of the levels shown occurs during a gap in observations (caused by instrument difficulties). In the following, we use trajectory calculations and techniques similar to those described by M95 to show evidence that this decrease is to a large extent caused by chemical processes.

## Data and Analysis

The MLS ozone data and retrievals are described by Froidevaux *et al.* [1994] and Froidevaux *et al.* [1995, submitted to *J. Geophys. Res.*]. Precisions (rms) of individual ozone measurements are  $\approx 0.2$ - $0.3$  ppmv, with absolute accuracies of 10-30% in the lower stratosphere. The ozone data are gridded at  $4^\circ$  latitude by  $5^\circ$  longitude using Fourier transform techniques that separate time and longitude variations [Elson and Froidevaux 1993].

Rossby-Ertel potential vorticity (PV) is calculated from United Kingdom Meteorological Office (UKMO) analyses [Swinbank and O'Neill 1994]. For vertical sections, PV is scaled in “vorticity units” ( $s^{-1}$ ) [e.g., Manney *et al.*, 1994b] to give a similar range of values at all levels.

The trajectory code [Manney *et al.*, 1994b] uses UKMO horizontal winds and diabatic descent rates from an independent radiation code. For forward trajectory calculations, parcels were initialized on a  $2^\circ$  latitude by  $5^\circ$  longitude grid (e.g., Fig. 2a) at selected isentropic levels throughout the stratosphere. As described by M95, an ozone mixing ratio is associated with each parcel on the initial day by interpolating

from the gridded MLS data. The subsequent motion of these tagged parcels (e.g., Fig. 2c) represents the expected behavior of ozone due solely to transport. This behavior is compared with the observed ozone interpolated to the parcels' positions on later days (e.g., Fig. 2b). M95 used this method with passive tracer data from the Cryogen Limb Array Etalon Spectrometer (CLAES), as well as MLS ozone, for the 1992-93 NH winter, showing that the trajectory calculations reproduced the main features of passive tracer evolution. Due to exhaustion of the CLAES cryogen, no passive tracer data are available from UARS for the 1993-94 winter. Even so, the previous success gives confidence that the present trajectory calculations can fairly accurately reproduce the effects of large scale transport.

M95 used three-dimensional binning and interpolation to grid the results from the trajectory calculations described above. Here, we use a reverse trajectory technique similar to that described by Sutton *et al.* [1994] to obtain gridded fields. Parcels are initialized throughout the NH on the grid used for the MLS data on each of the days we are interested in examining. The trajectory code is then run backwards in time to the initial day, 15 Feb 1994, and MLS ozone for 15 February is interpolated to the 15 February positions of the parcels started on a grid on each of the succeeding days. Thus, the calculated field on the initial grid shows the ozone mixing ratio that would be transported to those locations from the 3-d field for 15 February. This procedure requires more resources for the trajectory calculations, since a separate calculation must be done for each day of interest, but then requires only a simple interpolation from a gridded field to the parcel positions, rather than the complex binning and interpolation gridding procedure used by M95. Comparison of the two techniques showed very similar results for this case.

## Results

For parcels initialized at 465 K on 15 Feb 1994, the observed ozone at the parcel positions on 14 Mar 1994 in the vortex region (Fig. 2b) was considerably lower than that predicted by the trajectory calculation (Fig. 2c). Fig. 3 summarizes the results of these trajectory calculations throughout the time studied, showing the average, minimum, and maximum of observed ozone for all parcels started at 465 K that, on each day, have scaled  $PV \geq 1.4 \times 10^{-4} \text{ s}^{-1}$  (this contour is in the midst of the region of strong PV gradients, and thus all parcels within it are considered to be inside the vortex; the contour is indicated in Fig. 2). The open symbols show the corresponding ozone values from the trajectory calculation; thus, these change only when parcels move into or out of the region being averaged over. Fig. 3 shows similar trends for observed and calculated ozone during the first part of the period, but a marked decrease in observed ozone with respect to calculated ozone after the data gap. A similar plot (not shown) for parcels started at 840 K, in the middle stratosphere indicates very similar behavior of observed and calculated ozone in the vortex throughout the observing period. This suggests that, in a region where chemical changes are not expected, the trajectory calculation is reproducing the general evolution of ozone in the vortex.

Fig. 4 compares 465 K ozone maps from M1S observations, and as simulated using the reverse trajectory procedure described above, on 25 Feb and 14 Mar 1994. A slight increase in high values of calculated ozone in the vortex is seen on 25 Feb 1994. Much larger differences are seen between observed and calculated fields on 14 March, with the calculated field showing a significant increase as a result of diabatic descent bringing down higher ozone from above, but the observed field showing a decrease over the period. 9 March fields (not shown) show very similar amounts of vortex ozone to 14 March, indicating that most of the differences are in the behavior between 25 February and 9 March.

Vortex-averaged ozone from the trajectory calculation is shown in Fig. 5, using the

same display as Fig. 1b, which showed a time series of ~vortex-averaged MLS ozone. The calculated ozone shows a steady increase as larger ozone mixing ratios are transported to lower levels in the vortex; the increase is most rapid during the first half of the period. The observed behavior seen in Fig. 1 is inconsistent with the transport calculations at all levels shown in Fig. 5, and throughout most of the period. Fig. 6 compares the overall observed and calculated changes in ozone in the lower stratosphere between 15 Feb and 13 Mar 1994; differences are shown in PV/ $\theta$  space [e.g., Manney *et al.*, 1994a]. While the observed difference shows overall decreases in ozone in the lower stratospheric vortex (scaled PV  $\gtrsim 1.2 \times 10^{-4} \text{ s}^{-1}$ ) at all levels up to  $\approx 660 \text{ K}$ , the calculated field decreases only in a small region outside the vortex near 520 K, and a small region near the center of the vortex near 660 K.

The inconsistencies shown above between the behavior of the observed ozone and the ozone resulting from the trajectory calculation, together with the observed enhancement of ClO [Waters *et al.*, 1995], are strong evidence for chemical ozone depletion in the lower stratosphere during late February and early March 1994. In Fig. 7, we estimate the amount of chemical change that may have taken place at several levels in the lower stratosphere. Assuming that the calculated vortex-averaged ozone variations represent all changes in ozone due to dynamical processes, the difference between the observed and calculated variations then indicates the change in ozone due to non-dynamical (chemical) processes that would be required to produce the observed evolution. In Figs. 7b and 7c, little or no chemical depletion is required to explain the behavior of ozone at 520 K or 465 K in the early part of the period, while the observed lack of increase at 585 K suggests that downwelling may be masking some chemical depletion there. Later in the period, the amount of ozone destroyed by chemical processes at each of the levels shown may be as much as about twice the observed decrease between the beginning of the data gap and the end of the observing period. M95 found that the computed descent may at times be overestimated in the NH

winter. Thus, we regard our results as an upper limit on the amount of chemical ozone depletion.

## Conclusions

In the absence of distributed tracer data for diagnosing transport, three-dimensional trajectory calculations initialized with observed MLS ozone have been used to simulate the large-scale transport of ozone in the Arctic lower stratosphere from mid-February to mid-March 1994. Comparison of these simulations of transport-induced ozone with the observed ozone evolution provides strong evidence that substantial chemical ozone depletion occurred in the Arctic lower stratospheric vortex during late February and early March 1994. Throughout most of this period, diabatic descent is bringing higher ozone in from above, masking part of the chemical destruction of ozone; our calculations indicate that, over the two-week period of low temperatures in late February and early March 1994, the chemical depletion of ozone could have been nearly twice that suggested by the observed decrease in the lower stratosphere.

**Acknowledgments.** We thank the MLS team for their support, T. Luu for data management, P. Newman for supplying the original PV routines, the UKMO (A. O'Neill and R. Swinbank) for meteorological data. This work was part of a UARS Theoretical and Experimental investigations at the Jet Propulsion Laboratory, California Institute of Technology, and was done under contract with the National Aeronautics and Space Administration.



## References

- Elson, L. S., and L. Froidevaux, The use of Fourier transforms for asymptotic mapping: Early results from the Upper Atmosphere Research Satellite Microwave Limb Sounder, *J. Geophys. Res.*, 98, 23,039-23,049, 1993.
- Froidevaux, L., J. W. Waters, W. G. Read, L. S. Elson, D. A. Flower, and R. F. Jarnot, Global ozone observations from UARS MIS: An overview of zonal mean results, *J. Atmos. Sci.*, 51, 2846-2866, 1994.
- Larsen, N., B. Knudsen, I. S. Mikkelsen, I. S. Jorgensen, and P. Eriksen, ozone depletion in the Arctic stratosphere in early 1993, *Geophys. Res. Lett.*, 21, 1611-1614, 1994.
- Manney, G. L., and R. W. Zurek, Interhemispheric Comparison of the development of the stratospheric polar vortex during fall: A 3-dimensional perspective for 1991-1992, *Geophys. Res. Lett.*, 20, 1275-1278, 1993.
- Manney, G. L., L. Froidevaux, J. W. Waters, R. W. Zurek, W. G. Read, L. S. Elson, J. B. Kumer, J. L. Mergenthaler, A. E. Roche, A. O'Neill, R. S. Harwood, I. MacKenzie, and R. Swinbank, Chemical depletion of lower stratospheric ozone in the 1992-1993 northern winter vortex, *Nature*, 370, 429-434, 1994a.
- Manney, G. L., R. W. Zurek, A. O'Neill, and R. Swinbank, On the motion of air through the stratospheric polar vortex, *J. Atmos. Sci.*, 51, 2973-2994, 1994b.
- Manney, G. L., L. Froidevaux, J. W. Waters, and R. W. Zurek, Evolution of MIS ozone and the polar vortex during winter, *J. Geophys. Res.*, in press, 1995.
- Sutton, R. T., H. Maclean, R. Swinbank, A. O'Neill, and F. W. Taylor, High-resolution stratospheric tracer fields estimated from satellite [observations using Lagrangian trajectory calculations, *J. Atmos. Sci.*, 51, 2995-3005, 1994.
- Swinbank, R., and A. O'Neill, A Stratosphere-t roposphere data assimilation system, *Mon. Weather Rev.*, 122, 686-702, 1994.
- Waters, J. W., G. L. Manney, W. G. Read, L. Froidevaux, D. A. Flower, and R. F. Jarnot, UARS MIS observations of lower stratospheric ClO in the 1992-93 and 1993-94 Arctic

winter vortices, *Geophys. Res. Lett.*, in press, 1995.

Figure 1. (a) Minimum high-latitude UKMO temperatures (K) at 465 K from 15 Feb through 16 March 1994. (b) vortex-averaged MLS ozone (ppmv) from 15 Feb through 16 Mar 1994, from 4201 < (=100 hPa) to 655 K ( $\approx 20$  hPa); The “vortex-average” is an area-weighted average over the region with scaled PV  $\geq 1.4 \times 10^{-4} \text{ s}^{-1}$ . Contour interval is 0.2 ppmv, with 3.6 to 3.8 ppmv shaded.

Figure 2. Initial ozone (ppmv) at 465 K on 15 Feb 1994, and predicted and observed ozone at positions of parcels started at 465 K on 14 Mar 1994. Predicted values are the observed values at the parcel positions on 15 Feb, advected with the parcels. Observed values are interpolated to the parcel positions from the MLS data on each day. Most of the parcels shown are moving downwards during the run. The projection is orthographic, with 0° longitude at the bottom of the plot and 90°E to the right; dashed lines show 30° and 60° latitude circles. The  $1.4 \times 10^{-4} \text{ s}^{-1}$  contour of scaled PV at 465 K is overlaid on the plots.

Figure 3. The average (circles), minimum (triangles), and maximum (squares) values of ozone mixing ratio (ppmv) as computed by interpolating MLS data to the parcel locations determined by trajectory calculations (solid symbols) and as computed directly from the conserved initial ozone mixing ratios associated with these parcels (open symbols), for 15 Feb 1994 through 14 Mar 1994. The ensemble of air parcels used was initialized at 465 K and is constrained to have a scaled PV  $\geq 1.4 \times 10^{-4} \text{ s}^{-1}$  on the day considered.

Figure 4. Synoptic maps of ozone (ppmv) at 465 K from observations and trajectory calculations on 25 Feb and 14 Mar 1994. Layout is as in Fig. 2. PV contours in the region of strong gradients are overlaid on the plots of observed values; these contours are 0.2, 0.25 and  $0.3 \times 10^{-4} \text{ Km}^2 \text{ kg}^{-1} \text{ s}^{-1}$  ( $0.29 \times 10^{-4} \text{ Km}^2 \text{ kg}^{-1} \text{ s}^{-1}$  is equivalent to a scaled PV of  $1.4 \times 10^{-4} \text{ s}^{-1}$ ),

Figure 5. As in Fig. 1, but for calculated ozone.

Figure 6. Differences (ppmv) in (a) observed and (b) calculated ozone in the lower stratosphere (420 -740 K) between 13 Mar 1994 and 15 Feb 1994, as a function of scaled PV and 8; dashed lines indicate a decrease over the time period. Contour interval is 0.1 ppmv.

**Figure 7.** Observed (black line) and calculated (pale grey line) vortex-averaged ozone change (ppmv) at 585, 520, and 465 K, and estimated “non-dynamical” change (thick dark grey line) for 15 Feb through 16 Mar 1994.

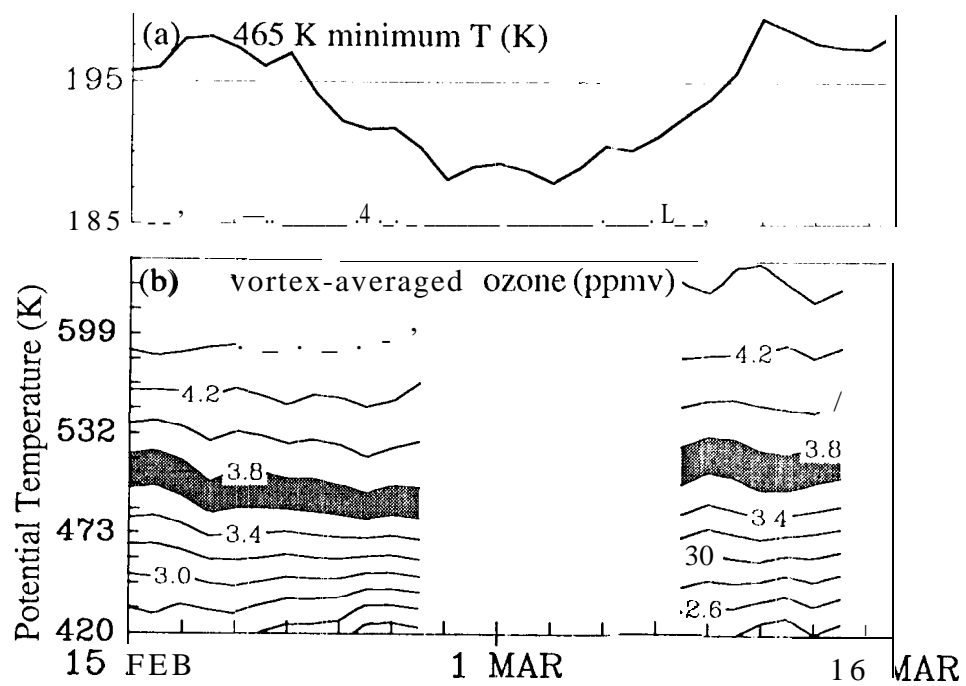


Fig. 1

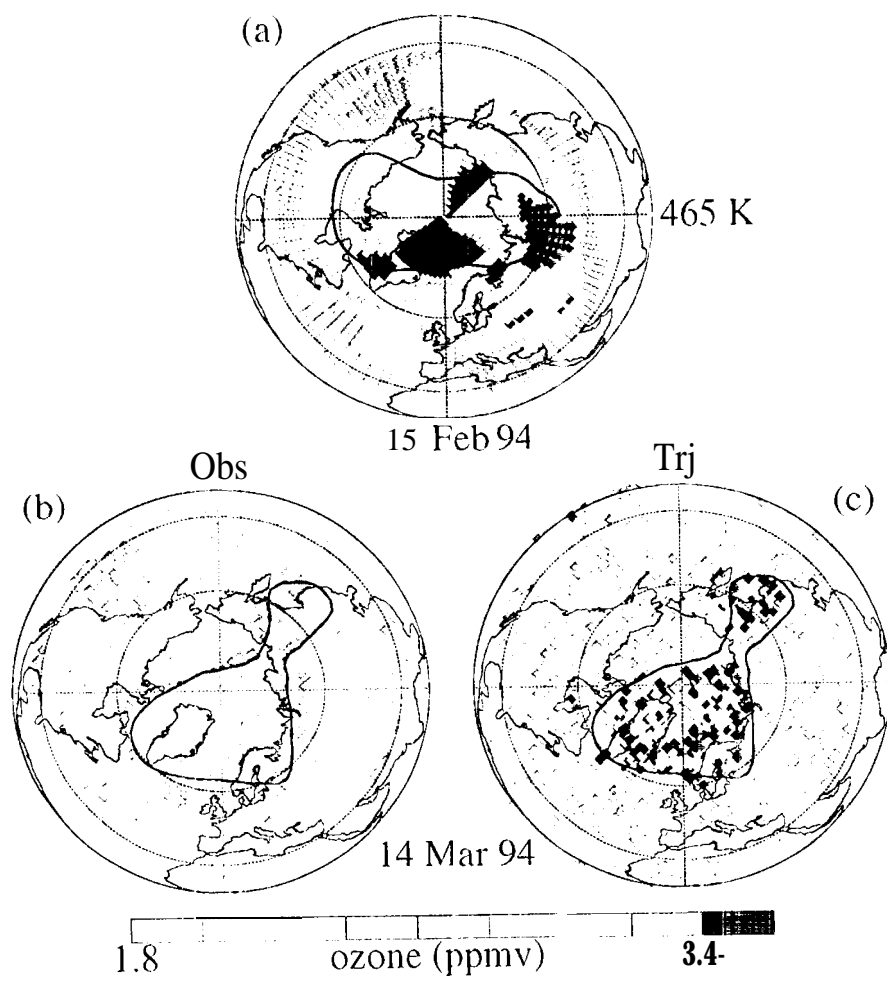


Fig. 2

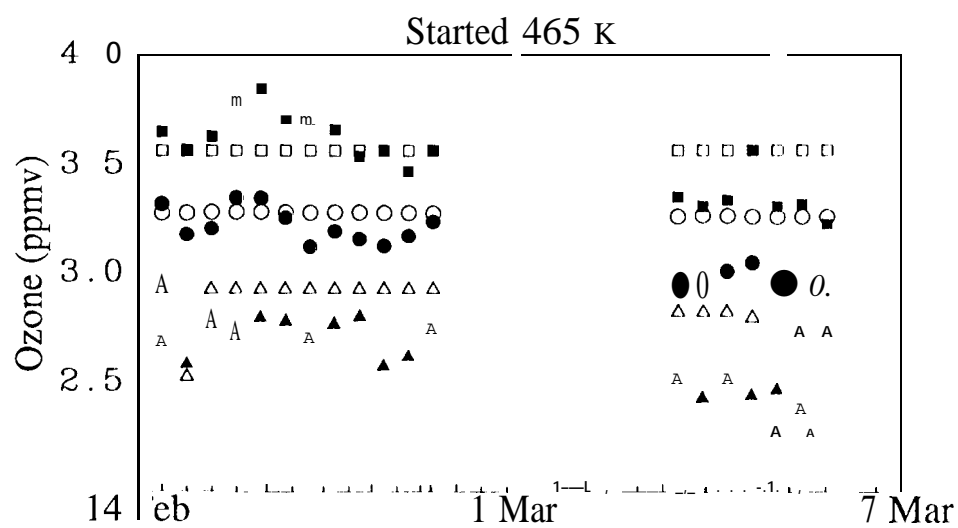


Fig. 3

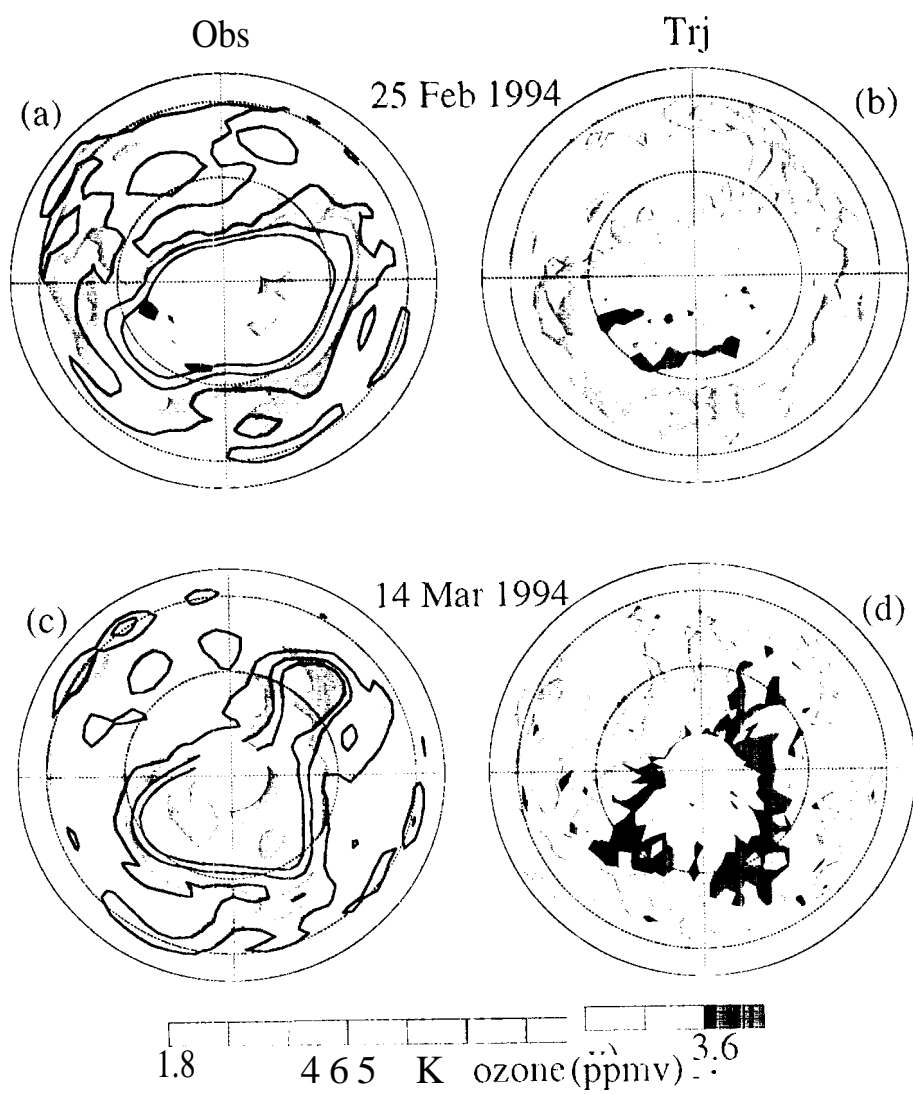


Fig. 4



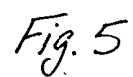


Fig. 5

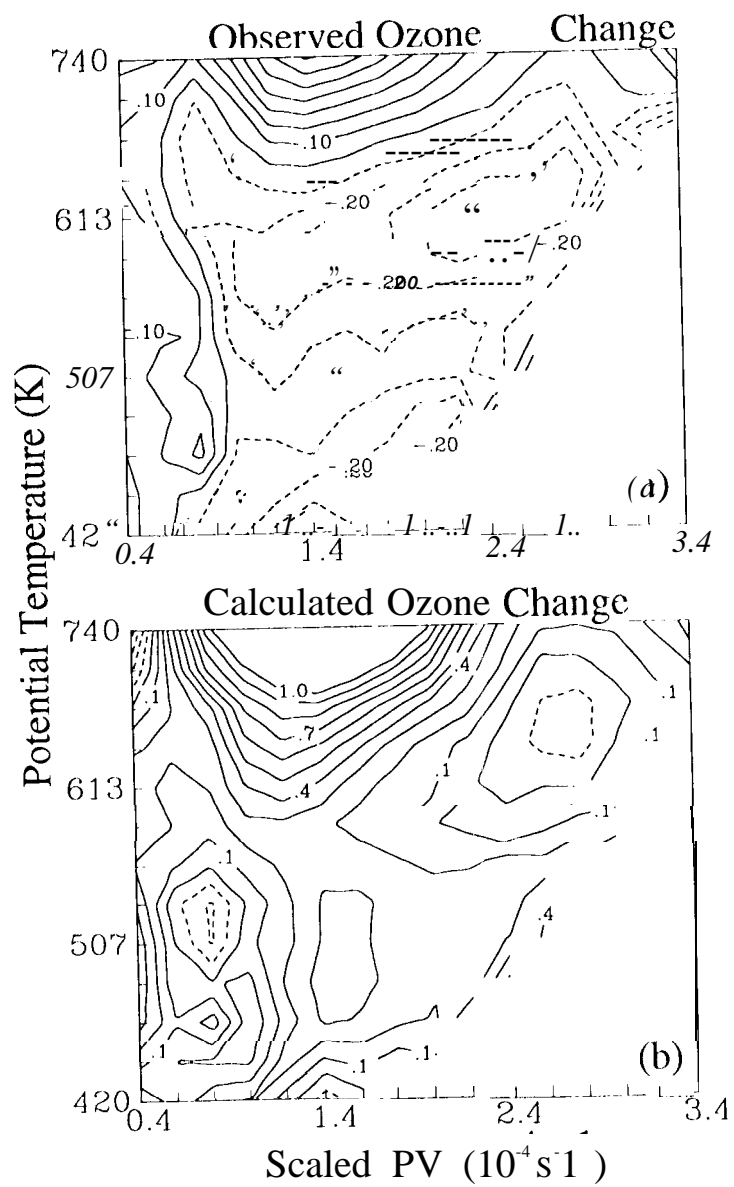


Fig. 6

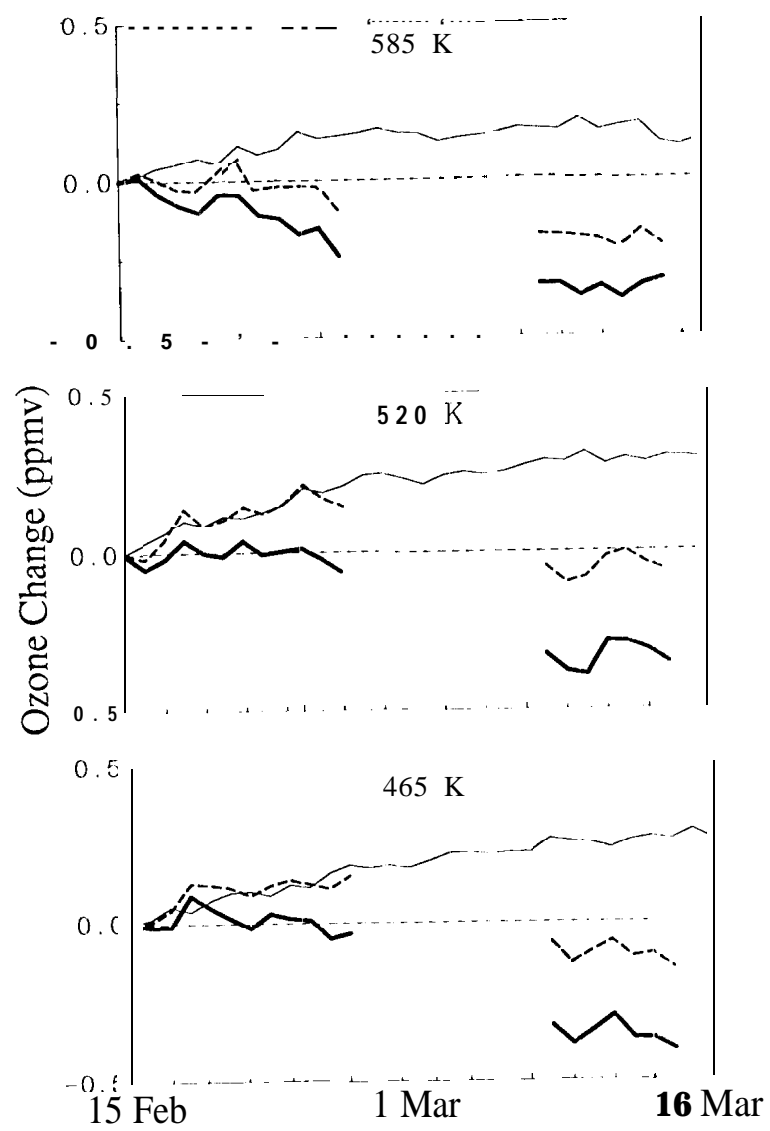


Fig. 7